Highly efficient H-β Fraunhofer line optical parametric oscillator pumped by a single-frequency 355 nm laser

Jian Ma (马 剑)[1,2], Tingting Lu (陆婷婷)[1], Xiaolei Zhu (朱小磊)[1,*], Xiuhua Ma (马秀华)[1], Shiguang Li (李世光)[1], Tianhua Zhou (周田华)[1], and Weibiao Chen (陈卫标)[1]

[1]*Key Laboratory of Space Laser Communication and Detection Technology, Shanghai Institute of Optics and Fine Mechanics, Chinese Academy of Sciences, Shanghai 201800, China*

[2]*University of Chinese Academy of Sciences, Beijing 100049, China*

**Corresponding author: xlzhu@siom.ac.cn*

Received April 9, 2018; accepted June 13, 2018; posted online July 27, 2018

A highly efficient laser system output at the H-β Fraunhofer line of 486.1 nm has been demonstrated. A high pulse energy single-frequency hybrid 1064 nm master oscillator power amplifier was frequency-tripled to achieve 355 nm laser pulses, which acted as the pump source of the beta barium borate nanosecond pulse optical parametric oscillator. With pump energy of 190 mJ, the laser system generated a maximum output of 62 mJ blue laser pulses at 486.1 nm, corresponding to conversion efficiency of 32.6%. The laser spectrum width was measured to be around 0.1 nm, being in conformity with the spectrum width of the solar Fraunhofer line.

OCIS codes: 190.4970, 190.2620, 140.3538, 140.7300.
doi: 10.3788/COL201816.081901.

Sea water has a transmission window in the range of the blue–green spectrum, which can be utilized for marine laser applications, including laser depth sounding, underwater laser communication, and ocean laser detection radar systems. The spectral attenuation coefficient varies in different types of seawater. A blue laser in the region of 450–495 nm is extremely suitable for deep ocean applications, while a green laser in the region of 510–550 nm is suitable for coastal seawater applications[1]. Compact solid-state blue–green pulsed lasers have attracted common attention for the advantages of high peak power and good beam quality. To date, high power frequency-doubled neodymium-doped yttrium aluminum garnet (Nd:YAG) 532 nm[2] green pulsed lasers have been greatly developed and widely applied in underwater laser communication systems[3] and airborne laser bathymetric charting systems[4,5]. Recently, pulsed blue lasers have also become a hot research point. In 2015, Leeuwen *et al.* reported on a *Q*-switched vertical-cavity surface-emitting laser (VCSEL) side-pumped Nd:YAG laser producing more than 1 W 473 nm blue output at 210 Hz with 4.9 mJ pulse energy and at 340 Hz with 3.2 mJ pulse energy[6]. In 2016, Creeden *et al.* obtained about 2 W of 486.5 nm light at a 500 kHz pulse repetition frequency by using a pulsed thulium-doped fiber laser as a pump source for a two-stage second harmonic generation (SHG) scheme[7]. However, the output laser peak power is insufficient to meet the application requirements in the existing blue pulsed lasers[8].

Furthermore, it is extremely attractive in ocean application systems if the central laser wavelength matches with Fraunhofer lines[9,10]. The system signal-to-noise ratio can be increased due to the reduced background[11,12]. The spectrum width of the Fraunhofer line is mostly too narrow to practically apply, which raises a high request for linewidth of the laser source, as well as the optical filter. In the blue–green region, there are mainly two Fraunhofer lines that are of interest: the H-β line at 486.13 nm with a spectrum width of 0.14 nm and the Mg line at 518.36 nm with a spectrum width of 0.16 nm[9,12]. These wavelengths of the Fraunhofer lines usually could not be obtained directly from the existing solid-state media.

Nonlinear frequency conversion technology[13] is an effective way to extend the laser wavelength[14]. Particularly, an optical parametric oscillator (OPO) could generate laser output with tunable wavelength[15]. A beta barium borate (BBO)-based OPO pumped by an ultraviolet (UV) laser could provide broad tunability from the blue laser to the mid-infrared laser[16,17].

In this article, a single frequency near-infrared pulsed laser with high pulse energy has been developed as the fundamental beam. Nonlinear crystals have realized the function of the frequency conversion process, including third harmonic generation (THG) and OPO. The fundamental pulsed laser is based on a 1064 nm hybrid master oscillator power-amplifier (MOPA) system, including both fiber laser amplifiers and laser diode (LD)-pumped solid-state laser amplifiers. The 1064 nm MOPA is frequency-tripled to 355 nm by two lithium triborate (LBO) crystal bulks. The 486.1 nm laser pulses at the H-β Fraunhofer line with single pulse energy of 62 mJ have been achieved based on an OPO pumped by the 355 nm laser. The laser peak power reached up to 7.7 MW, which could satisfy the need of long distance and large depth ocean applications.

The schematic diagram of the laser system's experimental setup is shown in Fig. 1. The laser system was combined by five modules, including the fiber pre-amplifier chain, the Nd-doped crystal pre-amplifier chain, the power-amplifier chain, the THG module, and the OPO. The former three modules constructed the 1064 nm hybrid

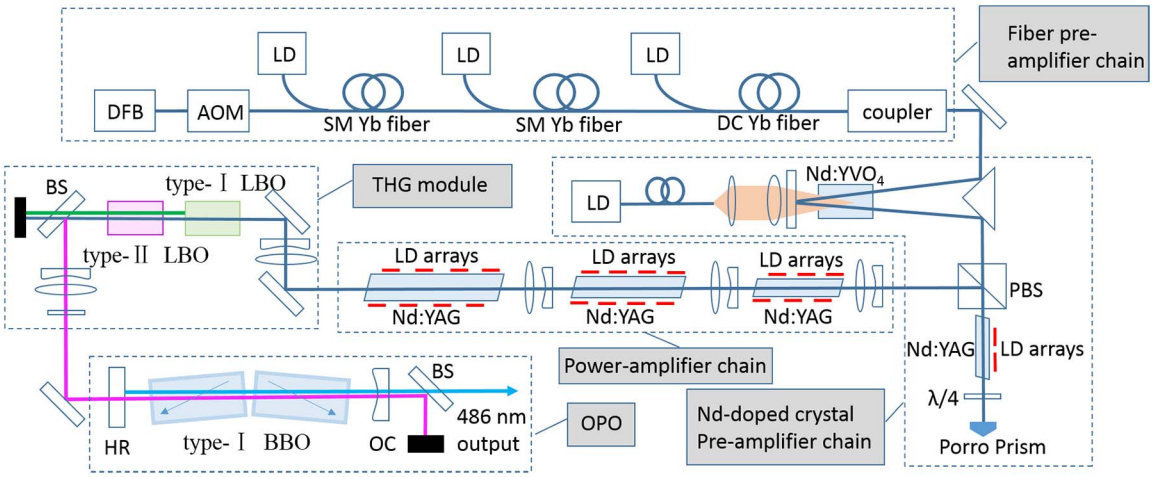

Fig. 1. Schematic diagram of the experimental setup.

MOPA, which is similar to the report in Ref. [18]. The difference is that the previous nonplanar ring oscillators (NPRO) seed laser was replaced by a 1064 nm distributed feedback (DFB) laser, owing to reliability and low intensity noise. The DFB seed laser with a linewidth of 2 MHz was chopped into nanosecond pulse sequence by an acousto-optic modulator (AOM). The pulsed seed laser was firstly amplified by two single-mode (SM) ytterbium (Yb)-doped fiber amplifiers (YDFAs) to suppress the amplified spontaneous emission (ASE) and then a double-cladding (DC) YDFA to enlarge the effective mode area. The pump sources of the fiber amplifiers were 976 nm continuous-wave (CW) LDs.

A 808 nm LD end-pumped double-pass Nd-doped yttrium orthovanadate (Nd:YVO_4) amplifier and a 808 nm LD side-pumped double-pass Nd:YAG zig-zag slab laser amplifier were employed as the high gain bulk pre-amplifier chain to amplify the laser pulse output from the fiber pre-amplifiers.

The high pulse energy power-amplifier chain consisted of three single-pass Nd:YAG zig-zag slab laser amplifiers side-pumped by 808 nm LD arrays. The pump light of the LD arrays is directly delivered into the gain medium to maximize the coupling efficiency. With increasing laser energy density in each stage, the aperture of the three Nd:YAG slabs enlarged successively together with beam expanding to decrease the risk of damage to the crystal.

The THG was realized by a type I phase matched LBO crystal and a type II phase matched LBO crystal. The type I LBO was cut at $\theta = 90°$, $\phi = 11°$ with dimensions of 10 mm × 10 mm × 15 mm for frequency-doubling of 1064 nm, and the type II LBO was cut at $\theta = 42.5°$, $\phi = 90°$ with dimensions of 10 mm × 10 mm × 15 mm for sum-frequency generation of 1064 nm and 532 nm. The output 355 nm laser pulses were employed as the pump source of the OPO. The polarization match of the OPO is shown as e (355 nm) → o (486 nm) + o (1313 nm). The OPO was singly resonant at the signal wavelength of 486 nm and operated in a linear plane-concave cavity consisting of a plane cavity mirror and a concave output coupler (OC). The plane cavity mirror was high reflection (HR) coated at a signal wavelength of 486 nm and anti-reflection (AR) coated at pump wavelength of 355 nm and idle wavelength of 1313 nm. The concave OC with curvature radius of 1 m was partly reflectively coated at 486 nm and AR coated at 355 nm and 1313 nm. Two of the same type I phase matched BBO bulks with a phase matching cut angle of $\theta = 29.6°$, $\phi = 90$ were employed as the parametric crystal. The effective nonlinear coefficient (d_{eff}) of BBO is 2.06 pm/V, and the walk-off angle of the pump light is 70.2 mrad. The BBO crystals were cross symmetrically placed relative to the pump beam axis to compensate for the walk-off effect[19]. The aperture of the BBO bulks was 8 mm × 8 mm. The BBO bulks were placed close enough to prevent back conversion to the pump radiation. Mounting of the BBO crystal was arranged to allow for rotation of the crystals in the phase matching plane to adjust the output signal wavelength.

After being modulated by the AOM, the 1064 nm seed laser pulses at 20 Hz with pulse duration of 20 ns were amplified gradually by the subsequent multi-stage hybrid amplifiers. Finally, maximum 500 mJ pulse energy of 1064 nm laser was obtained. The laser beam quality factor M^2 was measured to be smaller than 2.5 by a Spiricon M^2 200 beam analyzer, showing excellent beam quality at such high pulse energy output. The spectral characteristic of the amplified pulsed laser was measured by a HighFinesse Wavelength Meter WS7, and the linewidth was determined to be smaller than the 120 MHz measuring limit of the instrument. Pulse energy of 190 mJ at 355 nm with pulse width of 9.7 ns was obtained with sum-frequency conversion efficiency of 38%. Since a UV laser easily causes coating damage, the 355 nm pump beam size for the OPO was determined to be 4.5 mm in diameter, corresponding to the maximum pump peak power density of 123 MW/cm^2, which was proven to be safe for the optical thin film by experimentation.

The walk-off length of the parametric crystal is calculated to be 29 mm by

$$l_\omega = \frac{\sqrt{\pi}}{2}\frac{\omega_p}{\rho}\sqrt{\frac{\omega_p^2+\omega_s^2}{\omega_p^2+\omega_s^2/2}}, \tag{1}$$

where ρ is the walk-off angle, ω_p is the pump beam radius, and ω_s is the signal beam radius. Therefore, when the crystal length is smaller than the walk-off length, the crystal length can be considered as the effective gain length. In the OPO experimental setup, two different crystal lengths of 15 and 20 mm were taken into comparison.

In a same 60 mm long OPO cavity, the output pulse energy of the 486.1 nm blue laser with different BBO crystal lengths (15 and 20 mm) and output transmissions ($T_{\rm OC} = 20\%$ and $T_{\rm OC} = 30\%$) is shown in Fig. 2 as a function of the 355 nm pump pulse energy. The output energy increased linearly with the pump energy increasing, where no saturation occurred. Longer parametric crystals afford higher parametric gain, and, therefore, higher output energy was achieved by a 20 mm long BBO. The maximum conversion efficiency η in a singly resonant pulsed OPO is determined by

$$\eta = \frac{0.9(1-R)(\log N)^{2.33}}{[1-R(1-\delta_{\rm scat})]N}, \tag{2}$$

where R is the reflectivity of the OC, $\delta_{\rm scat}$ is the cavity scattering loss, and N is the ratio of the pump density to the threshold pump density. η is inversely proportional to reflectivity. Taking $\delta_{\rm scat} = 0.3$ and $N = 7.7$ into calculation, η was theoretically calculated to be 36% for $T_{\rm OC} = 30\%$ and 28% for $T_{\rm OC} = 20\%$, and thus higher conversion efficiency could be achieved with $T_{\rm OC} = 30\%$ than $T_{\rm OC} = 20\%$.

The threshold pump density was about 16 MW/cm^2 with $T_{\rm OC} = 30\%$. Maximum pulse energy of 62 mJ was achieved by two 20 mm long BBO crystals at 7.7 times the threshold pump density, corresponding to conversion efficiency of 32.6%. The output energy stability at maximum pulse energy was measured in 10 min, the standard deviation was calculated to be 1.41 with average output energy of 60 mJ, and the instability was 2.35%.

Figure 3 shows the near-field beam profile of the OPO output of the 486 nm laser measured by a Spiricon silicon CCD camera SP620 with maximum pulse energy. The beam profile shows it in good uniformity. The beam parameter product (BPP) at maximum output energy was measured to be BPP(x) = 2.4 mm · mrad and BPP(y) = 1.5 mm · mrad. According to the M^2-factor definition, $M^2 = (\omega\cdot\theta)/(\omega_0\cdot\theta_0) = {\rm BPP}/(\lambda/\pi)$, the M^2-factor was calculated to be $M_x^2 = 15.5$ and $M_y^2 = 9.7$.

In a high energy nanosecond pulsed OPO, the output high beam quality and high conversion efficiency are contradictory. Figure 4 shows the conversion efficiency, as well as the beam divergence angle, as a function of the OPO cavity length. Both the conversion efficiency and the beam divergence angle are inversely proportional to the cavity length. The far-field laser beam divergence angle (full angle) with the maximum pulse energy of 62 mJ in a 60 mm long OPO cavity was measured to be 8 mrad in the x direction, which is parallel to the walk-off orientation of the extraordinary pump light, and 6 mrad in the y direction, which is perpendicular to the walk-off orientation of the extraordinary pump light. The fair-sized

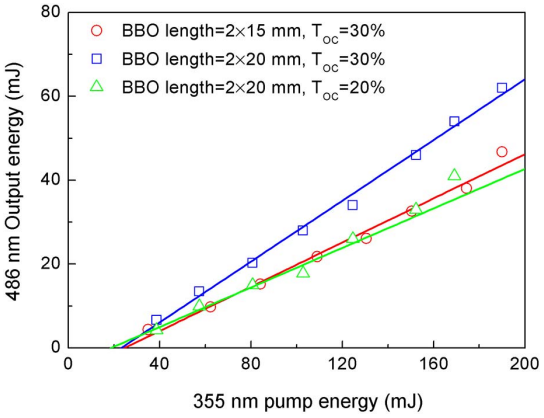

Fig. 2. Output 486.1 nm laser pulse energy as a function of the pump energy with cavity length of 60 mm.

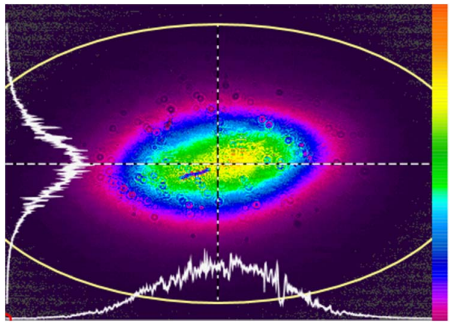

Fig. 3. Near-field beam profile of OPO output laser with pulse energy of 62 mJ.

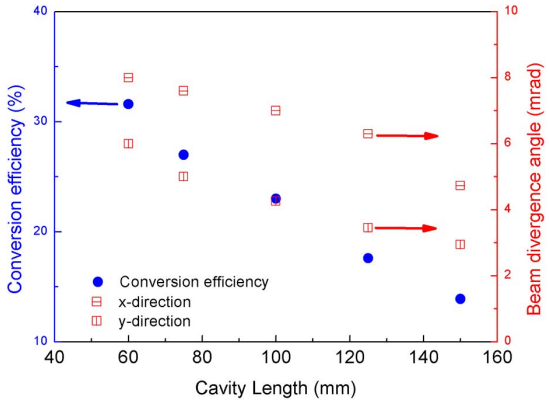

Fig. 4. Conversion efficiency and beam divergence angle as a function of the OPO cavity length.

output beam divergence angle results from the relatively large pump beam diameter of 4.5 mm and short cavity length. The difference of the beam divergence in two directions is caused by the noncollinear angle between the pump wave (extraordinary light) and the signal wave (ordinary light) in the phase matching plane. On one hand, short cavity length is advantageous to shortening the establishment time of the signal pulse and offset the enhancement of the pumping threshold by a large pumping spot for the purpose of preventing coating damage. On the other hand, the short cavity length and the large pump light spot size will lead to a large Fresnel number for the OPO cavity, which in turn will deteriorate the beam quality.

The pulse temporal profiles were detected by Si-based detectors and recorded by a Tektronix Oscilloscope MDO4104C. The pulse temporal profile of OPO output laser, as well as the pump pulse profile, is shown in Fig. 5. The pulse width of the OPO output laser was measured to be 8 ns with a smooth pulse shape, while the pump laser pulse width was about 9.7 ns. The maximum peak power of the 486.1 nm blue laser pulses reached up to 7.7 MW.

Figure 6 shows the spectral profile of the output blue laser referred to as the solar reference spectrum[20]. The spectrum of the blue laser was measured by the Yokogawa optical spectrum analyzer AQ6374. The central laser wavelength was measured to be 486.1 nm with maximum output energy and well-matched to the solar Fraunhofer H-β line. The spectrum width of the output laser was around 0.1 nm, less than the H-β linewidth of 0.14 nm[9]. In OPO operation, the output laser linewidth is related to the pump laser linewidth, the pump beam quality, the acceptance angle of the parametric crystal, and the cavity length fluctuation. In our experimental setup, the pump laser is frequency-tripled by single-frequency MOPA with excellent beam quality; also, the acceptance angle of BBO is small to benefit the spectrum performance. There is no active control of the cavity for the moment.

In summary, we have demonstrated a blue laser system at the wavelength of the H-β Fraunhofer line of 486.1 nm

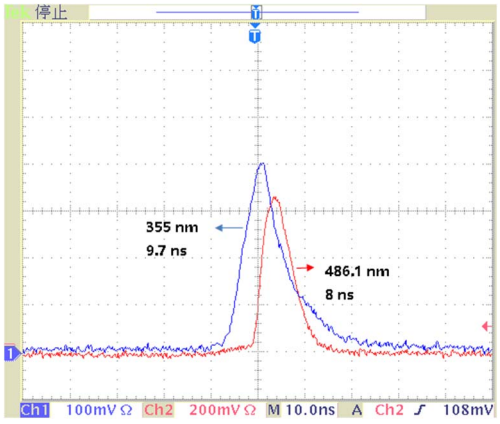

Fig. 5. Pulse temporal profiles of OPO pump laser and output laser.

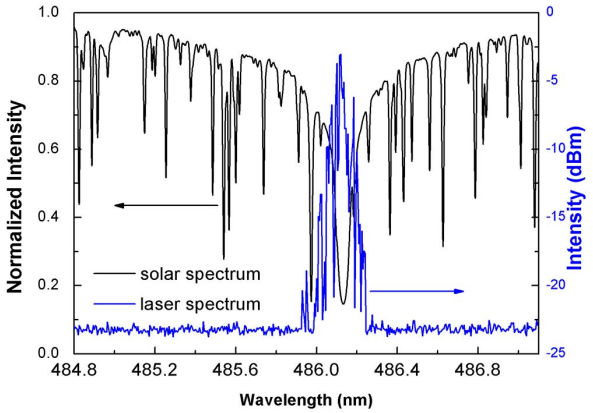

Fig. 6. OPO output laser spectrum and solar reference spectrum[20].

with spectral width less than the H-β linewidth. The output pulse energy of 62 mJ with high conversion efficiency was obtained in the BBO OPO pumped by a narrow linewidth 355 nm pulsed laser. Such a high energy Fraunhofer line pulsed laser may show great application prospects. The next study will be focused on improving the laser beam quality and further enhancement of the spectral properties.

This work was supported by the National Key Research and Development Program of China (No. 2016YFC1400902), the National Key Scientific Instrument and Equipment Development Project (No. 2013YQ120343), the Scientific Innovation Fund of Chinese Academy of Sciences (No. CXJJ-16S014), and the Development Program of China (No. 2014AA093301).

References

1. G. D. Ferguson, in *Proceedings of Ocean Optics IV* (1975), p. 150.
2. Y. B. Zheng, L. Ding, X. D. Zhou, R. S. Ba, J. Yuan, H. L. Xu, X. Y. Yang, B. Chen, J. Na, Y. J. Li, and W. G. Zheng, Chin. Opt. Lett. **14**, 051601 (2016).
3. E. Y. S. Young and A. M. Bullock, in *Proceedings of Free-Space Laser Communication Technologies XV* (2003), p. 146.
4. H. H. Kim, Appl. Opt. **16**, 46 (1977).
5. M. J. Sinclair, D. J. Stephenson, and R. M. Barker, in *Proceedings of Oceans 2003 MTS/IEEE* (2003), p. 770.
6. R. Van Leeuwen, T. Chen, L. Watkins, G. Y. Xu, J. F. Seurin, Q. Wang, D. L. Zhou, and C. Ghosh, in *Proceedings of Solid State Lasers XXIV: Technology and Devices* (2015), p. 9342.
7. D. Creeden, J. Blanchard, H. Pretorius, J. Limongelli, and S. D. Setzler, in *Proceedings of Fiber Lasers XIII: Technology, Systems, and Applications* (2016), p. 972829.
8. X. M. Liu, J. Laegsgaard, R. Iegorov, A. S. Svane, F. O. Ilday, H. H. Tu, S. A. Boppart, and D. Turchinovich, Photon. Res. **5**, 750 (2017).
9. M. G. Lovern, M. W. Roberts, S. A. Miller, and G. T. Kaye, in *Proceedings of Ocean Optics XI* (1992), p. 149.
10. G. Giuliano, S. Viola, S. Watson, L. Laycock, D. Rowe, and A. E. Kelly, in *Proceedings of 18th International Conference on Transparent Optical Networks* (2016), p. 1.
11. S. H. Wu, X. Q. Song, and B. Y. Liu, Remote Sens-Basel **5**, 6079 (2013).

12. G. Giuliano, L. Laycock, D. Rowe, and A. E. Kelly, Opt. Express **25**, 33066 (2017).
13. S. Z. Cui, L. Zhang, H. W. Jiang, and Y. Feng, Chin. Opt. Lett. **15**, 041402 (2017).
14. Z. C. Wang, F. Yang, S. Y. Xie, Y. T. Xu, J. L. Xu, Y. Bo, Q. J. Peng, J. Y. Zhang, D. F. Cui, and Z. Y. Xu, Appl. Opt. **51**, 4196 (2012).
15. X. H. Meng, Z. H. Wang, W. L. Tian, S. B. Fang, and Z. Y. Wei, Appl. Phys. B **124**, 9 (2018).
16. S. Wu, V. Kapinus, and G. A. Blake, Spr. Hdb. Aud. **5337**, 102 (2004).
17. R. Akbari and A. Major, Laser Phys. **23**, 035401 (2013).
18. X. B. Xie, D. K. Wei, X. H. Ma, S. G. Li, J. Q. Liu, X. L. Zhu, and W. B. Chen, Laser Phys. **26**, 055403 (2016).
19. M. Kaucikas, M. Warren, A. Michailovas, R. Antanavicius, and J. J. van Thor, Laser Phys. **23**, 025401 (2013).
20. K. Chance and R. L. Kurucz, J. Quantum Spectrosc. Ra **111**, 1289 (2010).